KfK 4906
August 1991

Estimation of the Temperature Structure Parameter and the Sensible Heat Flux from SODAR Measurements

H. Gentou, N. Kalthoff, P. Thomas, S. Vogt
Institut für Meteorologie und Klimaforschung

Kernforschungszentrum Karlsruhe

KERNFORSCHUNGSZENTRUM KARLSRUHE
Institut für Meteorologie und Klimaforschung

KfK 4906

Estimation of the Temperature Structure Parameter and the Sensible Heat Flux from SODAR Measurements

H. Gentou *, N. Kalthoff, P. Thomas, S. Vogt

* delegated from Remtech S.A., 2 and 4, avenue de l'Europe, B.P. 159 - 78143 Vélizy Cedex - France.

Kernforschungszentrum Karlsruhe GmbH, Karlsruhe

Als Manuskript gedruckt

Kernforschungszentrum Karlsruhe GmbH
Postfach 3640, 7500 Karlsruhe 1

ISSN 0303-4003

Abstract

A commercially available Doppler–SODAR and a sonic anemometer–thermometer have been operated during June and July 1990 at the Nuclear Research Center Karlsruhe to measure backscattered echo, the wind vector, the standard deviation of the vertical wind speed and sonic data like the heat flux. Other meteorological parameters have additionally been measured by the SODAR, the sonic instrument at 100 m AGL, and at a 200 m high tower at which the sonic instrument was installed.

Temperature structure parameters derived from SODAR backscattered echo and from sonic anemometer-thermometer data using mixed layer similarity relationship are compared and show fairly good correlation.

Measurements of the SODAR backscattered echo and standard deviation of the vertical wind speed are each used to estimate the sensible heat flux in the convective Planetary Boundary Layer. Comparison with simultaneous point measurement by the eddy correlation method shows good agreement between the two instruments.

Bestimmung des Temperaturstrukturparameters und des Stroms fühlbarer Wärme mit einem SODAR.

Zusammenfassung

In den Monaten Juni und Juli 1990 wurden im Kernforschungszentrum Karlsruhe ein Doppler–SODAR und ein Ultraschall–Anemometer–Thermometer parallel betrieben. Das SODAR lieferte das Rückstreuecho, den Windvektor und die Standardabweichung der vertikalen Windgeschwindigkeit, das Ultraschall-Gerät den fühlbaren Wärmestrom. Weitere meteorologische Parameter wurden an einem 200 m hohen Meßmast sowie vom Ultraschall–Gerät gemessen, das sich in 100 m Höhe am Mast befand.

Unter Verwendung von gültigen Ähnlichkeitsbeziehungen in der konvektiv durchmischten Planetarischen Grenzschicht (PBL) wurde der Temperaturstukturparameter aus dem SODAR–Rückstreuecho und aus Ultraschall–Daten abgeleitet und verglichen. Es ergaben sich zufriedenstellende Übereinstimmungen.

Zur Bestimmung des Stroms fühlbarer Wärme in der konvektiven PBL dienten Rückstreuecho und Standardabweichung der vertikalen Windgeschwindigkeit. Vergleiche mit gleichzeitig durchgeführten Punktmessungen (Ultraschall–Instrument), die auf der Eddy–Korrelations–Methode beruhen, zeigen gute Übereinstimmung mit Parametern, die auf SODAR Messungen beruhen.

Contents

List of Figures

List of Tables

1 Introduction

Following a period of research, and development, SODARs are now widely used for environmental monitoring in a routine base. They are mainly used to measure vertical profiles of velocity, turbulence parameters such as the standard deviation σ_w of the vertical wind speed or the standard deviation σ_θ of the direction, and the backscattered echo amplitude, which are important for pollution studies and Planetary Boundary Layer (PBL) studies. Although the measurement of σ_w and σ_θ by SODAR is only moderately accurate (Chintawongvanich, 1989; Thomas and Vogt, 1990), the estimation of turbulence parameters by SODAR has advantages in some particular cases, as for example, over complex terrain, in that it gives a value averaged in space which is much less sensitive to local variation than the estimation by *in situ* sensors.

Monostatic SODARs can be used to detect regions of strong echos frequently associated with elevated inversions that trap pollutants beneath them. Kaimal *et al.* (1982) have shown that it is possible to evaluate the mixing height z_i using the backscattered echo amplitude of monostatic SODARs. Monostatic SODARs, when properly calibrated, are also able to measure the temperature structure parameter C_T^2, which is directly related to the temperature fluctuation, an essential piece of information in the study of the propagation of electromagnetic waves through a turbulent atmosphere.

Weil *et al.* (1980), and Coulter and Wesely (1980) have derived the sensible heat flux H from SODAR measurements in the convective PBL, with the use of the similarity theory. Their investigations show that SODARs give reasonable estimates of the sensible heat flux. However, the parameters estimated with the help of the similarity theory cannot be more accurate than the theory itself. As the equations derived from the similarity theory are based on empirical laws, adapted to results with best fit coefficents, they have some limitations.

During the summer 1990, a field test program was conducted at the Kernforschungszentrum-Karlsruhe (KfK) Institut für Meteorologie und Klimaforschung (IMK) to evaluate the capabilities of a commercially available SODAR, manufactured by the French enterprise REMTECH, to determine turbulence parameters. In Gentou *et al.* (1991), it was shown that σ_w and the characteristic scales of turbulence measured and calculated by SODAR and sonic anemometer compared well. In order to investigate further capability of SODARs to measure turbulence parameters within the PBL, we have studied two new topics, and here present a summary of the results.

In the first part, C_T^2 measured by a sonic anemometer–thermometer at 100 m above ground level (AGL) is compared to SODAR backscattered echo power, with the help of similarity relationships. This comparison makes it

possible to calibrate the SODAR echo.

In the second part, different methods to determine the sensible heat flux H at the surface from SODAR data are presented, and compared to eddy correlation measurement by a sonic anemometer-thermometer. Finally, a test is performed to check the validity of the two relationships derived from similarity theory.

2 Determination of C_T^2 by a Doppler-SODAR

2.1 Introduction

The temperature structure parameter C_T^2 is related to the temperature fluctuation and reflects the behaviour of the temperature spectrum in the inertial subrange. One of its main application is the study of propagation of optical waves in the atmosphere.

Many authors have presented comparisons of C_T^2 measured by monostatic SODARs and temperature turbulence probes (Asimakopoulos *et al.* , 1975; Haugen and Kaimal, 1978; Moulsley *et al.* , 1982; Asimakopoulos *et al.* , 1983; Keder et al, 1989). Haugen and Kaimal (1978) compared simultaneous measurements at three heights above ground. Their analysis indicated that the comparison factor between the SODAR echo and *in situ* sensors was a function of height and stability. Significant variations in SODAR calibration has been attributed to excess attenuation (Haugen and Kaimal, 1978; Clifford and Brown, 1980). Neff (1978) suggested that this excess attenuation, varying with frequency, wind speed, and antenna characteristics could reduce C_T^2 by a factor of 4. Asimakopoulos *et al.* (1983) measured C_T^2 in the first 100 meters above ground level with two small high frequency SODARs and observed no excess attenuation when calculating C_T^2 via the spectral method, using a fast response sensor.

Measurements of C_T^2 are not easy, especially in convective situations, because vertical plumes create inhomogeneities and disturb the temperature field. Moulsley *et al.* (1982) studied the influence of temperature anisotropy on the measurement of C_T^2. They suggested that the vertical temperature difference could contain some contributions from large scale inhomogeneous or anisotropic features in the temperature field. They presented results indicating typical overestimations by a factor of 2 when measuring C_T^2 using spaced temperature sensors. A study presented by Helmis *et al.* (1983) shows that, even in an isotropic temperature field, the C_T^2 measured along the wind direction and along a vertical direction are not equal. Furthermore, the ratio between the temperature structure parameter calculated via the temperature spectrum and via spaced temperature sensors varied between 0.75 in stable conditions and 3.4 in unstable to neutral conditions, with an average value about 2.0 .

Because no high response C_T^2 sensor was mounted on the meteorological tower during the experiment, the reference C_T^2 is calculated via similarity theory (Wyngaard *et al.* , 1971) with sonic anemometer data. The relationship of Wyngaard *et al.* is valid only in convective situations in the PBL. Thus, the comparison is possible only during such atmospheric situations.

The results reported in Section 2.4 are obtained from values of SODAR and sonic anemometer-thermometer averaged over half an hour and

measured during summer 1990 in an experiment at Karlsruhe. The data presented here have been carefully selected to avoid periods of shadowing of the sonic sensor by the tower.

2.2 Theory

2.2.1 SODAR C_T^2 measurement

The cross–section of backscattered acoustic power from a monostatic SODAR, expressed per unit solid angle, and per unit volume is, for a dry atmosphere,

$$\sigma = 0.0072\lambda^{-1/3}\frac{C_T^2}{T^2} \tag{1}$$

with λ the acoustic wavelength, and T the mean temperature in the scattering volume. The backscattered power as received by the SODAR is given by

$$\frac{P_r(R)}{S_r} = [P_t\ S_t][\frac{c\tau}{2}][(D/R^2\ G)][e^{-2\alpha R}\ L_x]\sigma \tag{2}$$

where

P_r measured received electrical power

S_r efficiency of antenna system in converting received acoustic to electrical power

P_t transmitted electrical power

S_t efficiency of antenna system in converting emitted electrical to acoustic power

c speed of sound

τ duration of transmitted sound pulse

D effective antenna aperture

R travel distance to scattering volume of interest

G aperture gain factor

α molecular attenuation coefficient

L_x excess attenuation coefficent

σ cross–section of backscattered acoustic power per unit solid angle, and per unit volume.

In order to obtain absolute measurements, the SODAR has to be calibrated acoustically (Asimakopoulos *et al.* , 1983), and the molecular attenuation has to be computed as a function of height from *in situ* measurements of temperature, pressure and humidity. The excess attenuation is the term used for loss of acoustic intensity due to refraction by the wind (Neff, 1978; Moulsley and Cole, 1980) and beam broadening by turbulence. Refraction results in a change in the angle of arrival of the backscattered sound which gives rise to loss of received intensity due to the lower sensitivity of the receiving antenna to off-axis beams. Beam broadening by turbulence is less well understood at the present time (Clifford and Brown, 1980). We have not corrected data for the excess attenuation because the effects of spatial and temporal variations in the structure parameter cannot be easily included in the model presented by Clifford and Brown (1980).

In addition to these errors, the moisture fluctuations contribute to scattering. The effect is significant in very moist environments such as clouds, fog, or after heavy rain. However, we have neglected this contribution in our investigations, as such situations have been rare during June and July 1990.

2.2.2 Reference C_T^2 measurement

When convection is the dominant mechanism generating turbulence, the PBL has a well defined structure with three major components: the surface layer (approximately the lowest 10% of the PBL), the mixed layer (the middle 20%-70%), and the interfacial layer. Within the mixed layer the potential temperature, wind speed and wind direction profiles remain constant, due to intensive vertical mixing.

For local free convection, Wyngaard *et al.* (1971) have shown that the profile of C_T^2 can be described in the surface layer by Monin-Obukov's similarity theory. In these particular conditions, C_T^2 is proportional to $z^{-4/3}$, z being the altitude above ground level (AGL). This relationship seems also to fit quite well to data in the convective PBL (see Caughey and Palmer, 1979; Kaimal *et al.* , 1976; Coulter and Wesely, 1980). Kaimal *et al.* (1976) show that this relationship is valid to as high as half the height of the mixing layer, which may in turn be as high as 2 km during summer afternoons.

In the absence of direct measurement devices, we used this indirect calibration method based on the following equation (Wyngaard *et al.* , 1971):

$$C_T^2 = 2.68\Big(H/\rho c_p\Big)^{4/3}\Big(\frac{T}{g}\Big)^{2/3} z^{-4/3} \qquad (3)$$

where H is the sensible heat flux ($W\,m^{-2}$), ρ is the density of air ($1.2\,kg\,m^{-3}$), T is the temperature (K), g is the acceleration due to gravity ($9.81\,m\,s^{-2}$), and c_p is the specific heat of air at constant pressure ($c_p \approx 1005\,J\,kg^{-1}\,K^{-1}$).

Kaimal *et al.* (1976) studied the evolution of the sensible heat flux and the inversion base during the day. Their conclusion suggested that the sensible heat flux increases slowly during morning hours. The inversion base or mixed layer increases rapidly during the same time. Examination of data during the evening transition indicates that the inversion base remains nearly the same before sunset. But, at the same time, the sensible heat flux decreases very quickly and crosses zero about one hour before sunset. This study indicates that it is necessary to compare data on a reduced time interval between sunrise and sunset.

Coulter and Wesely (1980) proposed a correction factor for Eq.(3) which takes into account humidity fluctuations:

$$C_T^2 = 2.68\left(H/\rho c_p\right)^{4/3}\left(\frac{T}{g}\right)^{2/3} z^{-4/3}(1+0.007/\beta)^{4/3} \tag{4}$$

where β is the Bowen ratio. For β, we estimated an average value of 0.5 which is typical for a forest.

We have approximated $H/\rho c_p$ by $\overline{w'T'}$, the heat flux measured at 100 m AGL by the sonic anemometer-thermometer. All the data given by the sonic and the tower instruments are averaged and stored each 10 min. A correction of $\overline{w'T'}$ is performed following Schotanus *et al.* (1983):

$$\overline{w'T'} = \left(\overline{w'T'}_s + 2\frac{TU}{c^2}\overline{u'w'}\right)\left(1+\frac{0.51Tc_p}{\lambda\beta}\right)^{-1} \tag{5}$$

where T is measured by the temperature sensor of the meteorological tower at 100 m, $\overline{u'w'}$ and $\overline{w'T'}_s$ are measured by the sonic, c_p is the specific heat at constant pressure, and λ is the latent heat of condensation (for water, $\lambda \approx 2.510^6 J\,kg^{-1}$). To compare the sonic data to the SODAR data, the 10 min data, after this correction, are averaged over 30 min.

2.3 Experimental method

Since the KfK SODAR compensates the effect of spherical divergence of the acoustic waves, Eqs. (1) and (2) suggests that

$$C_T^2 \approx A^2\, L_\alpha^{-1} \tag{6}$$

with $L_\alpha = e^{-2\alpha z}$ being the molecular attenuation, and A the echo amplitude given by the SODAR. We have neglected the variations of temperature and considered the molecular attenuation being constant and equal to 0.75 dB/100 m (Harris 1966). Through the remainder of this report, the SODAR echo amplitude E has been corrected for molecular attenuation, following

$$E(z) = A(z)\, e^{\alpha z}. \tag{7}$$

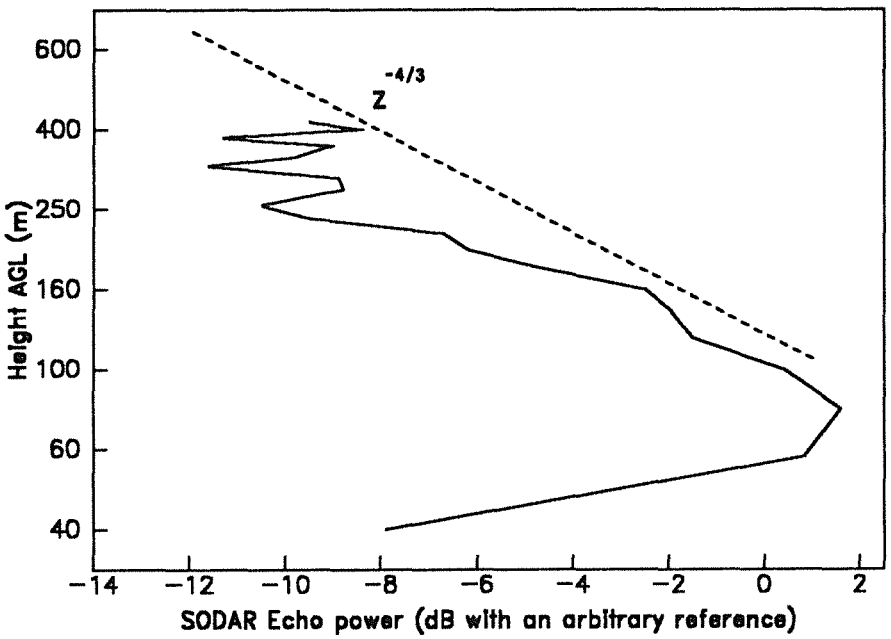

Figure 1: SODAR echo power E^2 versus altitude above ground level in log-log scales.

We obtain thus a simple proportionality coefficient m between C_T^2 and the SODAR echo power E^2. m can be estimated by the slope of the best fit-line between SODAR E_i^2 and sonic $C_{T\ i}^2$ with zero intercept :

$$m = \frac{\sum_{i=1}^{N} C_{T\ i}^2\ E_i^2}{\sum_{i=1}^{N} E_i^2\ E_i^2} \tag{8}$$

Since Eqs.(3) and (6) are true in the convective PBL, SODAR echo power is used to check if C_T^2 is proportional to $z^{-4/3}$. Therefore, a fit of $\log(E^2)$ against $\log(z)$ should also show a -4/3 slope. Figures 1, 2, and 3 give three examples of backscattered power profiles. The dotted lines indicate -4/3 slope.

In Figure 1, the coefficient of the echo power regression line is always smaller than -4/3, which could be interpreted as excess attenuation. In Figure 3, the peak of E^2 at about 300 m indicates the position of the mixing level or capping inversion. In Figure 1, 2, and 3, the echo at 40 m is underestimated because the SODAR electronic board is saturated.

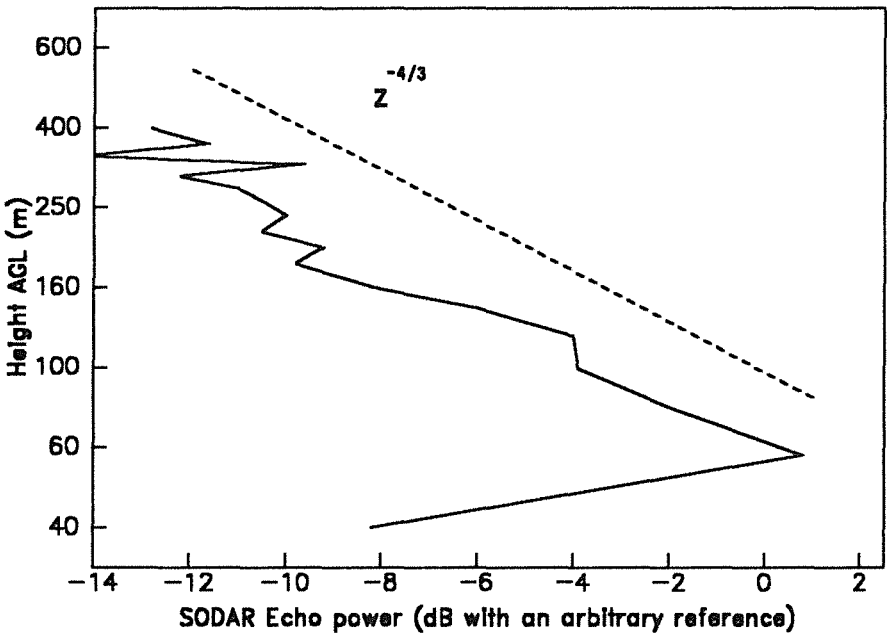

Figure 2: SODAR echo power E^2 versus altitude above ground level in log-log scales.

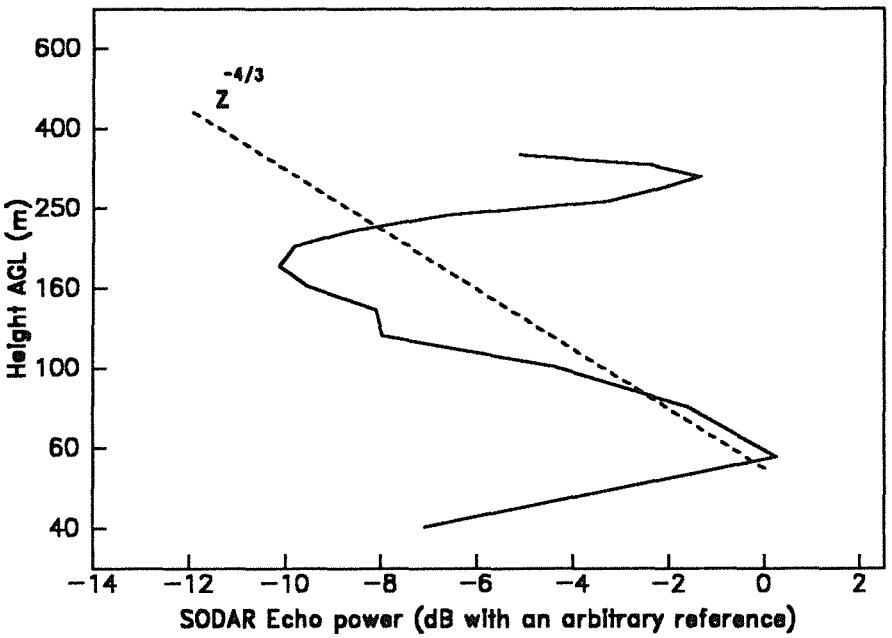

Figure 3: SODAR echo power E^2 versus altitude above ground level in log-log scales.

To caculate the calibration coefficient, the following criteria must be met:

- The atmospheric conditions must be convective. To check it, a test is performed in three steps: (i)We check if there is a saturation at 60 m, 80 m, 100 m. The lowest height with no saturation is the minimum height z_{min}; (ii) We calculate the fit of $\log(E^2)$ against $\log(z)$ between z_{min} and 180 m; (iii) If the SODAR power echo profile gives a slope between -1.66 and -1.1, the atmospheric condition is convective. If not, we go back to step (ii) with z between z_{min} and 250 m, or between z_{min} and 320 m. Then, the reference C_T^2 is calculated via Eq.(3) using sonic data.

- The time must be between 10h30 and 18h30 CET (Central European Time).

- The horizontal wind speed at 100 m is smaller than 12 ms^{-1}.

The -4/3 law is checked first for the smallest height interval to reduce errors introduced by excess attenuation or other problems of measurement of C_T^2 at high altitudes.

2.4 Results

2.4.1 Limitations of the theory

Data from June 1990 are used in Eq.(8) to calculate the calibration factor m of approximately 8.1×10^{-8}.

In order to investigate the reliability of this procedure, we make some tests with another data set, corresponding to July 1990. The scatter plot of SODAR echo power E^2 versus sonic C_T^2 measured in July 1990 is depicted in Figure 4. The regression line corresponding to the calibration factor $m = 8.1 \times 10^{-8}$ is also shown. The comparison in Figures 4 (and Figure 5, see below) reveals a large scatter. The SODAR overestimates C_T^2 at small values and underestimates C_T^2 at large values. Possible explanations of this phenomenon are as following: When the C_T^2 is very small, the SODAR fails to measure, the corresponding small values are not used in the 30-min average echo, and it is shifted to higher than actual average value. When C_T^2 magnitude is very large, the SODAR echo is underestimated because the SODAR electronic board is saturated. Thus, the 30-min average echo is shifted to smaller value, introducing an underestimation of C_T^2.

In view of the investigation of Kaimal et al (1976), we have plotted in Figure 6 the ratio of SODAR to sonic C_T^2 versus daytime. It is clear that the error in measurement by the SODAR is greater during the morning and evening. This is the reason why the calibration was performed with data within the time interval 10h30 to 18h30 (CET).

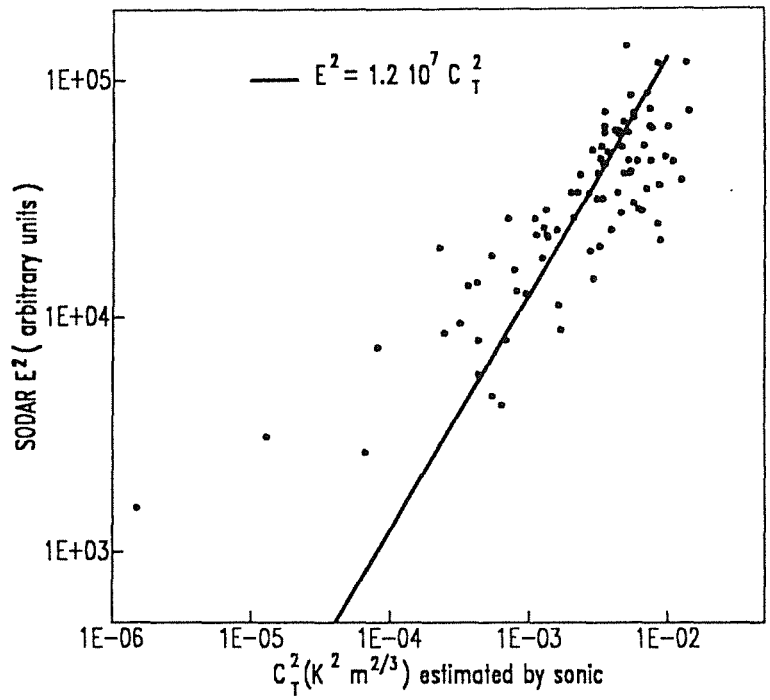

Figure 4: SODAR echo power E^2 versus sonic C_T^2 during July 1990.

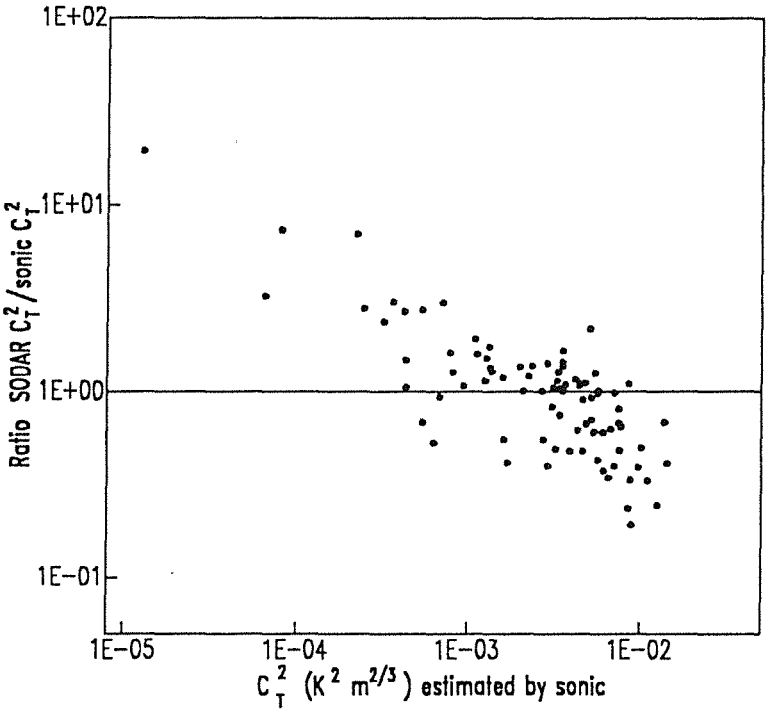

Figure 5: $C_T^{2\ SOD}/C_T^{2\ SON}$ versus $C_T^{2\ SON}$ during July 1990.

Figure 7 illustrates the scatter plot of the ratio of SODAR to sonic C_T^2 versus horizontal wind speed, measured by the sonic anemometer at 100 m AGL. The excess attenuation is expected to increase with increasing horizontal wind speed, resulting in an underestimation of C_T^2 by SODAR. However, there is no clear tendency towards increasing errors with increasing wind speed, up to 10 $m\,s^{-1}$.

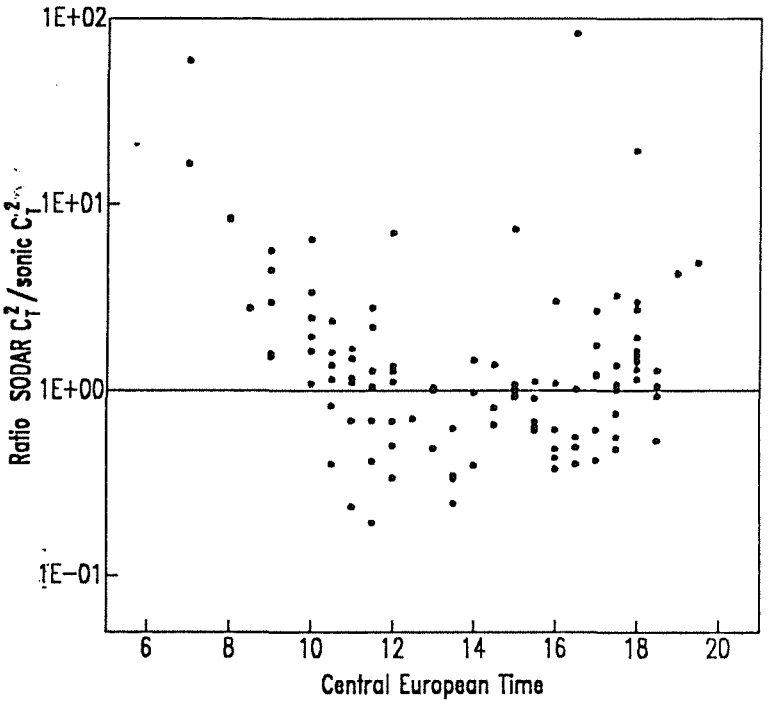

Figure 6: $C_T^{2\ SOD}/C_T^{2\ SON}$ versus time of day (CET) during July 1990.

2.4.2 Table of results

Only data within the limitations presented in Section 2.3 are used for the intercomparison. Table 1 summarizes the results for the months June and July. The overall accuracy of the SODAR C_T^2 measurements is estimated by calculating the bias and standard deviation of the logarithm of sonic and SODAR data.

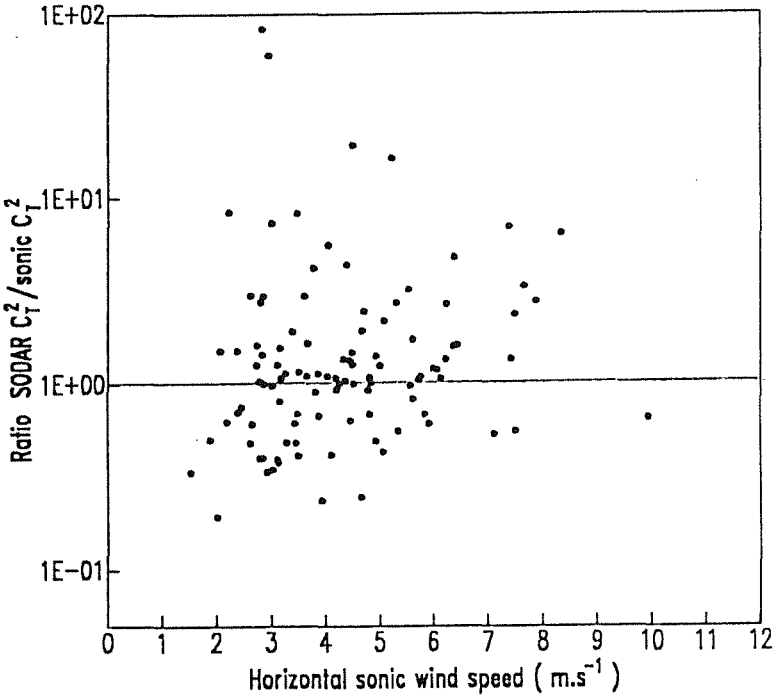

Figure 7: $C_T^{2\ SOD}/C_T^{2\ SON}$ versus the sonic horizontal wind speed during July 1990.

We have used logarithm of the temperature structure function because the variations of C_T^2 are typically of a magnitude of 100 to 1000, and are then better represented in logarithmic scales. The error criteria F and σ are given by

$$\log(F) = \frac{1}{N}\sum_{i}^{N}\log(C_{T\ i}^{2\ SON}/C_{T\ i}^{2\ SOD}) \tag{9}$$

$$\log(\sigma) = \Big[\frac{1}{N}\sum_{i}^{N}[\log(C_{T\ i}^{2\ SON}/C_{T\ i}^{2\ SOD}) - \log F]^2\Big]^{1/2} \tag{10}$$

giving

$$F = \prod_{i=1}^{N}\Big(\frac{C_{T\ i}^{2\ SON}}{C_{T\ i}^{2\ SOD}}\Big)^{1/N} \tag{11}$$

and the interval bounded by F/σ and $F\,\sigma$. The correlation R is also calculated with logarithms of the temperature structure function. The correlation is fairly good during the two months. It should be noted that other authors found similar results. For example, Asimakopoulos *et al.* (1983) found a correlation factor of 0.73 at 50 m AGL for C_T^2 averaged over a 1 h period.

Table 1: Comparison of C_T^2 measured by SODAR and sonic .

	Number N of points	F	Interval $[F/\sigma, F\,\sigma]$	R
June 1990	119	0.87	0.50-1.52	0.76
July 1990	87	0.97	0.42-2.24	0.84

2.4.3 Time series

We have plotted concatenated time series of C_T^2 measured during June and July 1990.

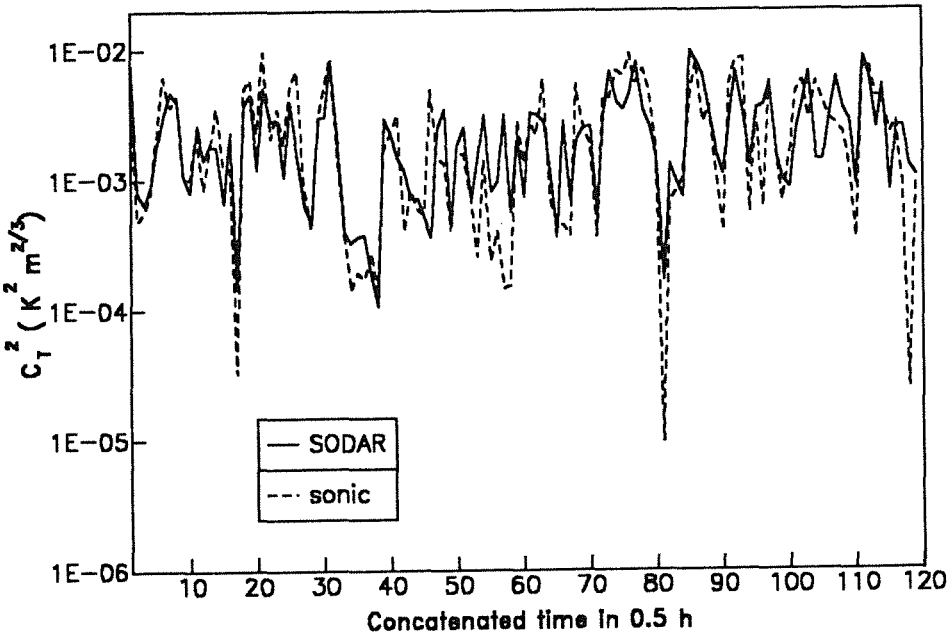

Figure 8: Concatenated time series of SODAR and sonic C_T^2 during June 1990.

Only data underlying the limitations presented in Section 2.3 are plotted. As expected, the time series of both instruments follow the same trend. But C_T^2 measured by SODAR is in most cases underestimated for large values and overestimated for small values.

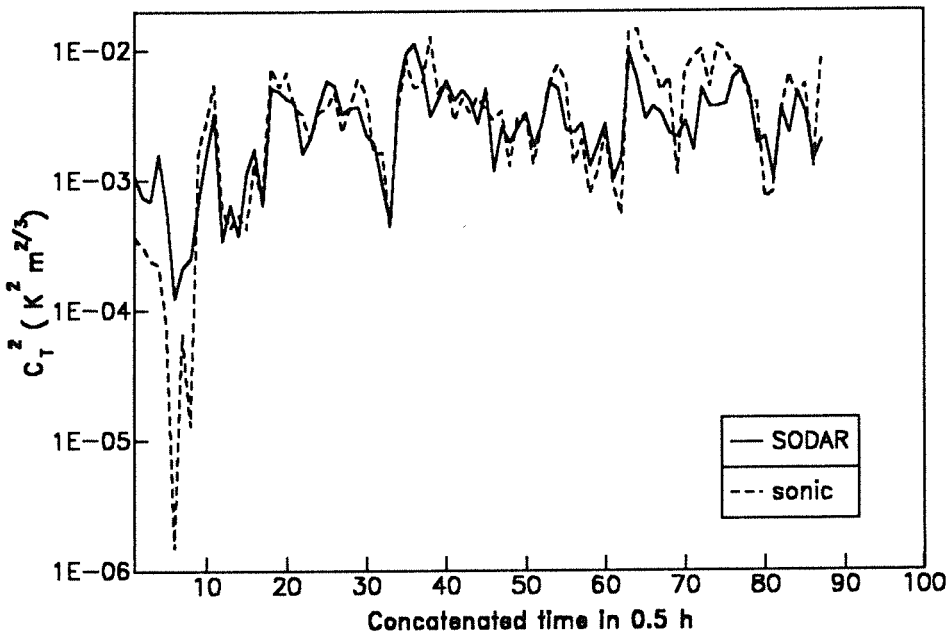

Figure 9: Concatenated time series of SODAR and sonic C_T^2 during July 1990.

2.5 Concluding remarks

There has been a number of comparisons of *in situ* measurements of C_T^2 with estimates of C_T^2 derived from SODARs. Neff and Coulter (1986) in their review paper indicated that it is probably unrealistic to expect to obtain C_T^2 better than within a factor of 2. Since vertical profiles of C_T^2 range over two orders of magnitude and since C_T^2 varies widely during daytime and nighttime, C_T^2 estimated by SODAR is still useful.

Our comparison shows that C_T^2 measured by SODAR is fairly well correlated to C_T^2 measured by sonic. Typical errors are within a factor of 2 under convective situations. One should keep in mind that our sonic C_T^2 was measured at a distance of 200 m from the SODAR by an indirect method. Considering these restrictions, it was not possible to obtain a very accurate reference C_T^2.

3 Sensible heat flux

3.1 Introduction

Estimations of the sensible heat flux in the surface layer are usually obtained from *in situ* one point sensors. However for meteorological studies over a large inhomogeneous area, a network of point measurements would be necessary. A system which can give a spatial average is often more convenient because it can be easily deployed and gives mean results representative of large volumes of the atmosphere in the PBL. Some fundamental work has been done by Weil *et al.* (1980), and Coulter and Wesely (1980). The intention in both cases was to use mixed layer similarity laws to obtain an estimate of the sensible heat flux from C_T^2 or σ_w measured by SODAR.

3.2 Sensible heat flux estimated by eddy correlation method

The turbulent flux $\overline{w'T'}$ was measured at 100 m AGL by the sonic anemometer-thermometer. After a correction following Equation (5), the sensible heat flux was then directly computed from

$$H_{ec} = \rho\, c_p\, \overline{w'T'}, \tag{12}$$

with "ec" indicating eddy correlation.

The measurement was taken rather high (100 m AGL), but the site is located in a pine forest. The average height of the pines is about 20 to 30 m and a measurement at 100 m AGL is high enough to assume that the surface elements did not cause a serious disturbance.

3.3 Sensible heat flux estimated by means of SODAR C_T^2

It has previously been shown that the SODAR can estimate relatively well C_T^2 at 100 m during convective situations. Thus, the SODAR can also be used to calculate the sensible heat flux. For forward propagation of optical or acoustic waves, the structure constant for refractivity fluctuation C_n^2 has been shown by Coulter and Wesely to be related to C_T^2, and T, by :

$$C_n^2 = \frac{C_T^2}{4T^2}\Big(1 + (0.06/\beta)^2\Big). \tag{13}$$

The term $(0.06/\beta)^2$ is a correction for the humidity fluctuations. Modifying the relationship of Wyngaard *et al.* (1971), Coulter and Wesely computed the sensible heat flux $H_{C_T}^{SOD}$

$$H_{C_T}^{SOD} = 0.48\, \rho\, c_p \left(g/T\right)^{1/2} \left(2\,T\,C_n\right)^{3/2} z\, \gamma_{so}, \tag{14}$$

with

$$\gamma_{so} = [1 + (0.07/\beta)^2]^{3/4}\, [1 + (0.06/\beta)^2]^{-3/4}\, [1 + 0.07/\beta_s]^{-1}. \tag{15}$$

β is the Bowen ratio at 100 m and β_s is the Bowen ratio on the ground. A first approximation of γ_{so} is

$$\gamma_{so} = \left(1 + 0.07/\beta_s\right)^{-1} \tag{16}$$

with β_s equal to 0.5 (see Section 2.2.2). The temperature was measured on the tower at 100 m, and the same value is used for all the levels. It is expected that in the well mixed layer, the potential temperature remains constant with altitude (Kaimal *et al.* , 1976). Thus, errors in measurement of T between 100 m and 300 m should be about 2 K or 0.7 %, which can be neglected.
Following results of Section 2,

$$C_T^2 \approx 8.1 \times 10^{-8} E^2, \tag{17}$$

with $T \approx 290\ K$ and $\beta \approx 0.5$. This gives

$$C_n \approx 5.0 \times 10^{-7} E. \tag{18}$$

The use of Eq.(14) for time periods when the atmosphere is not convective or when the mixing height is rapidly changing may lead to errors. As indicated in Section 2, only cases between 10h30 and 18h30 are included in the time series for intercomparison (steady state conditions). To check if the atmosphere is convective, we have used a method similar to the method presented in Section 2. If the comparison of the data with a -4/3 slope was satisfactory, the line maintaining the required -4/3 slope and providing the best fit to the data was used to estimate the sensible heat flux. The extent of the -4/3 slope varied from case to case.

3.4 Sensible heat flux estimated by means of σ_w

From similarity theory, Weil *et al.* (1980) have shown that in a well mixed layer where the mechanical production is negligible,

$$\sigma_w^2 \approx \delta \left(z \frac{g}{\theta_v} \overline{w'\theta_v'} \right)^{2/3} \tag{19}$$

where

- δ is a constant approximately equal to 1.4
- $\frac{g}{\theta_v}\overline{w'\theta_v'}$ is the local buoyancy production
- g is the acceleration due to gravity
- θ_v' is the virtual potential temperature pertubation

- w' is the vertical velocity perturbation

Therefore, in a dry convective layer, we have

$$\overline{w'T'} = \delta^{-3/2}\left(\frac{T}{g}\right)\left(\frac{\sigma_w^3}{z}\right) \tag{20}$$

In the well mixed layer, the sensible heat flux decreases linearly with height. Therefore, the sensible heat flux H follows the linear relationship:

$$H\left(1-\frac{z}{h'}\right) = \delta^{-3/2}\,\rho\,c_p\left(\frac{T}{g}\right)\left(\frac{\sigma_w^3}{z}\right). \tag{21}$$

yielding the following informations:

- the profile of the sensible heat flux in the well mixed adiabatic layer,
- the sensible heat flux at the surface by extrapolation of the linear part of the profile to $z = 0$,
- the height h' at which heat flux vanishes by linear extrapolation.

Large positive deviations of the sensible heat flux estimated by this method should be expected when the mechanical production is not negligible.

In previous studies (Gentou *et al.* , 1991; Chintawongvanich, 1989), the comparison of σ_w^{SOD} with *in situ* measurements showed that the SODAR underestimates large σ_w values, particulary during the daytime. This underestimation of σ_w is mainly due to the incomplete coverage of the vertical wind speed spectrum. Data taken during the summer 1990 Karlsruhe experiment have shown that the σ_w^{SOD} may be corrected using

$$\sigma_w = 1.07\,\sigma_w^{SOD} + 0.08 \quad (ms^{-1}). \tag{22}$$

Since the frequency of the spectral maximum changes only slightly in the mixed layer with height, we expect that in most cases, Eq.(22) will be a good approximation in the range 80 m–500 m.

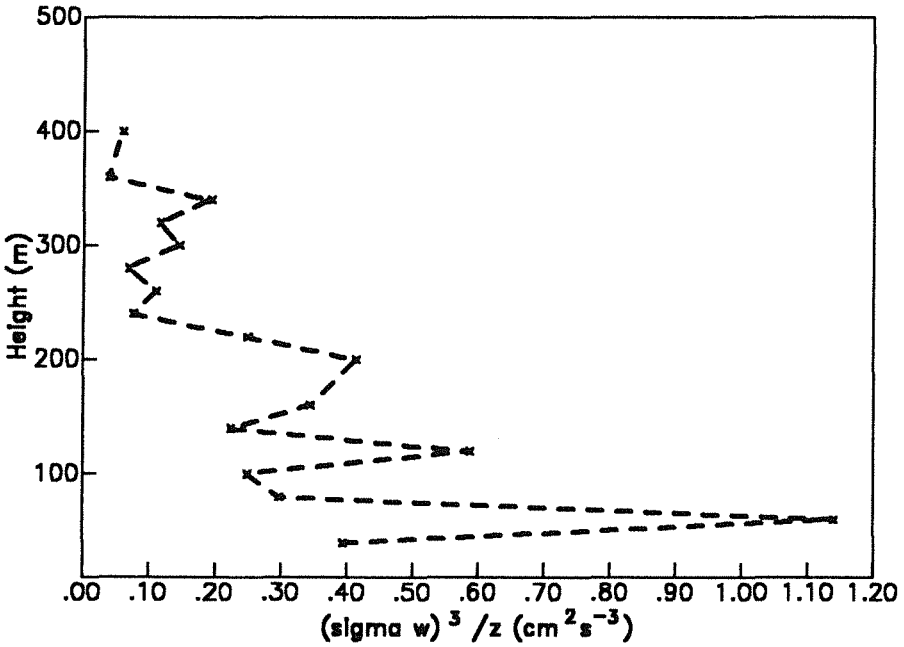

Figure 10: σ_w^3/z profile against z measured by SODAR.

Figure 10 illustrates a typical profile of σ_w^3/z. Although the profile fluctuates, a linear trend is present which is characteristic for the convective mixed layer. Two explanations are possible for these fluctuations: (i) the SODAR introduces errors in the measurement of σ_w , (ii) the inhomogeneities in the atmosphere introduce scatter in the linear σ_w^3/z profile.

To estimate the sensible heat flux, the following criteria must be met:

- The atmospheric conditions must be convective. To check it, a test is performed in two steps: (i) we calculate the fit of σ_w^3/z profile against z between 100 m and 200 m; (ii) if the fit of the σ_w^3/z profile against z gives a correlation between -1 and -0.8, the atmospheric condition is assumed to be convective. The intersection of the fit line with $z = 0$ gives the estimate $H^{SOD}_{\sigma_w - pr}$ of the sensible heat flux. The index "pr" stands for profile and refers to Eq.(21). If not, we go back to step (ii) with z between 100 m and 280 m, or between 100 m and 380 m.

- The time must be between 07h30 and 19h30 CET (Central European Time).

Following Eq.(20), estimates of the sensible heat flux at 100 m are also given by σ_w of the SODAR and sonic at 100 m AGL. These estimates are notated $H^{SOD}_{\sigma_w-100}$ and $H^{SON}_{\sigma_w-100}$, respectively. $H^{SON}_{\sigma_w-100}$ is measured at the same point as H_{ec}, the reference sensible heat flux and gives a direct estimation of the validity of the method of Weil *et al.* (1980) as sonic σ_w is supposed to be measured without errors.

3.5 Results

The heat flux values calculated from the respective sensors should not be expected to agree on a point to point basis for several reasons:

- The SODAR responds to a volume average, the sonic anemometer–thermometer responds to a point in space.
- The two sensors are 200 m apart and the topography, which is not homogeneous (see description in Gentou *et al.* , 1991), perturbs the turbulent eddies.

3.5.1 Limitations of the theories

(a) Limitations of the C_T^2 law

As previously presented, the hypothesis of a -4/3 law of the C_T^2 profile against z is true under steady state conditions and free convection. Melas *et al.* (1990) showed that the influence of stability is important: when the stability parameter z_i/L varies between -4.5 and 0, the relative error varies between 3 and 11. z_i is the mixing height and L is the Monin-Obukov's length. The sensible heat flux is greatly overestimated and the error increases with increasing stability. Furthermore, the occurence of the -4/3 slope does not imply necessarily free convection during early morning and late afternoon. In view of this, Coulter and Wesely (1980) studied the evolution of the ratio $H^{SOD}_{C_T}/H_{ec}$ during the day. They showed that the SODAR overestimates H during mornings and underestimates H during evenings. Figures 11 and 12 illustrate the ratio $H^{SOD}_{C_T}/H_{ec}$ in logarithmic scale versus the time of day in Central European Time (CET) for values of H_{ec} greater than 10 Wm^{-2}. The variation of the ratio is the lowest between 14h00 and 18h00 (CET), corresponding to the time interval when the theory is expected to apply, because the atmosphere at this time remains in a quasi steady state.

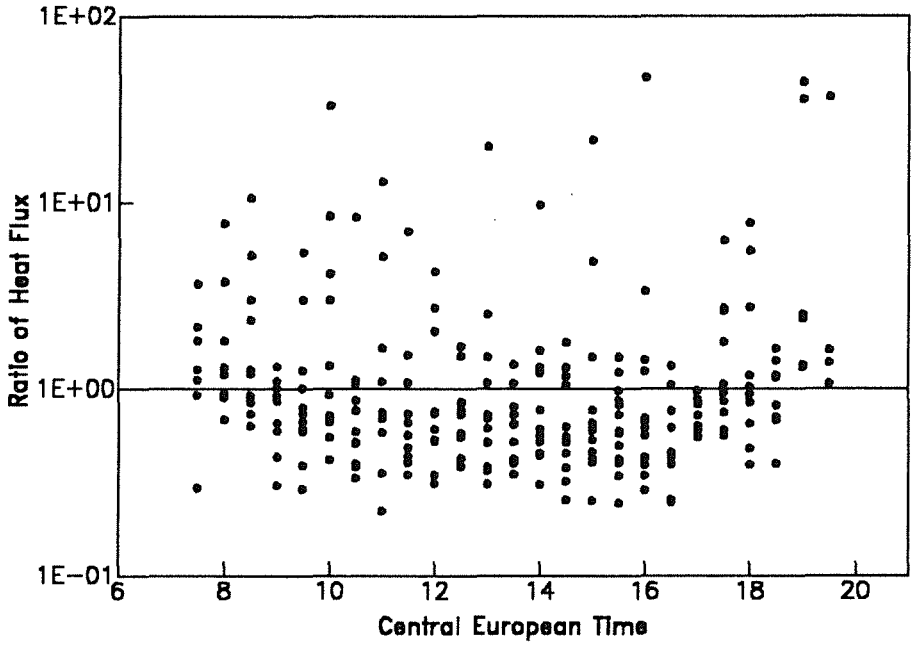

Figure 11: $H_{C_T}^{SOD}/H_{ec}$ versus time of day (CET) during June 1990.

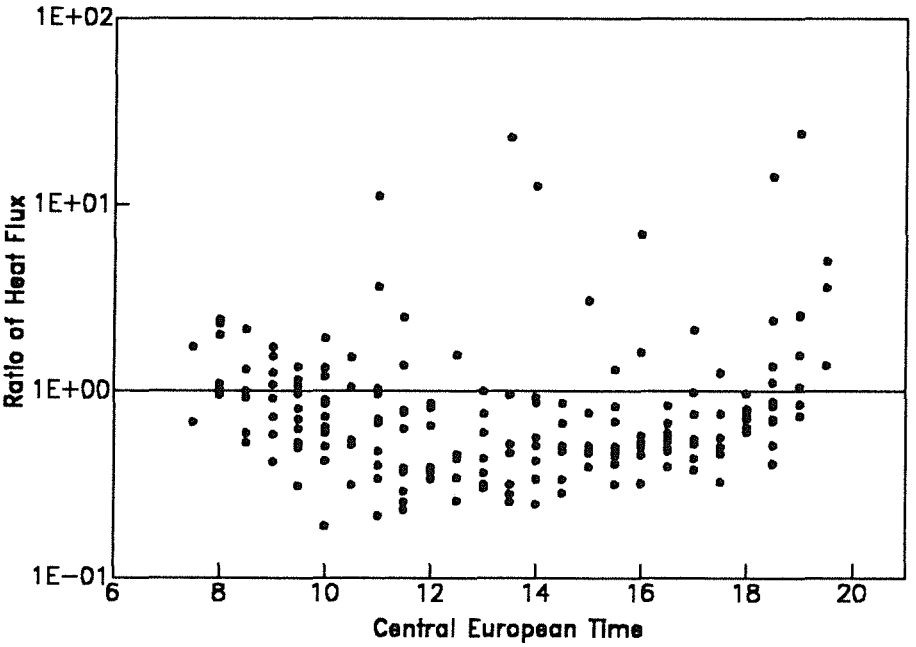

Figure 12: $H_{C_T}^{SOD}/H_{ec}$ versus time of day (CET) during July 1990.

(b)Limitations of the σ_w law

To study the hypothesis of Weil *et al.* (1980), we have calculated the relative error $(H^{SON}_{\sigma_w-100} - H_{ec})/H_{ec}$ as a function of σ_w for values of H_{ec} greater than 10 Wm^{-2}. Examining Figure 13, we find that for small σ_w ($\sigma_w <$ 0.65 $m\,s^{-1}$), the relative error is between 0 and 2. For $\sigma_w > 0.65\ m\,s^{-1}$, the relative error is always positive and can reach very large values. Under such conditions, the assumption of negligible local mechanical production is likely to be incorrect. However, as can be seen in Figure 13, a large σ_w value does not necessarily introduce large errors in the sensible heat flux estimation. Therefore, we have introduced a limitation in the evaluation of H by means of σ_w: When the standard deviation of vertical wind speed is greater than 1.1 ms^{-1}, the estimate of sensible heat flux will be computed with 1.1 ms^{-1} instead of σ_w.

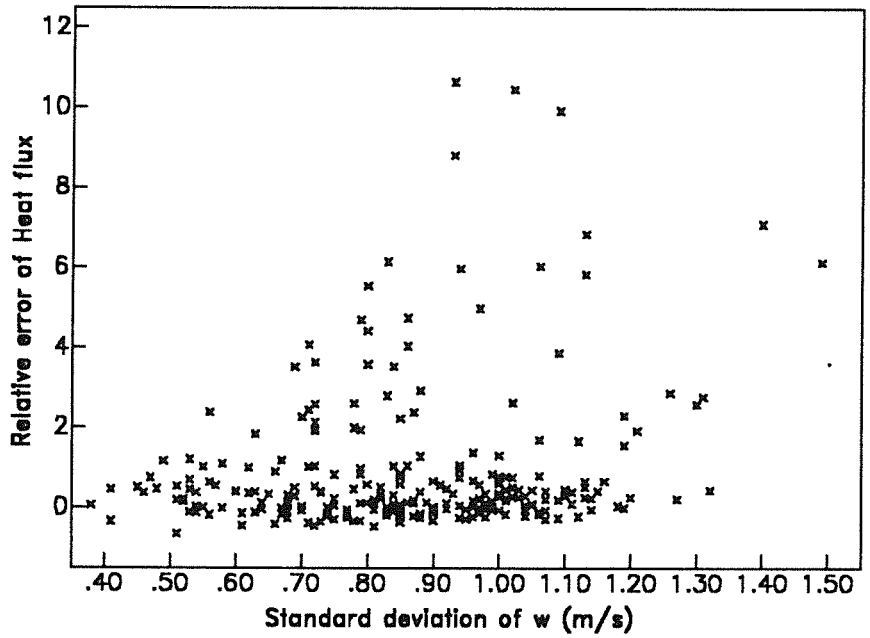

Figure 13: $(H^{SON}_{\sigma_w-100} - H_{ec})/H_{ec}$ versus sonic σ_w during July 1990.

We have also calculated the local mechanical production

$$-\overline{u'w'}\,\frac{dU}{dz},$$

with the mean wind shear dU/dz measured by using tower wind data at 80 m and 130 m, and the momentum flux $\overline{u'w'}$ measured by the sonic. Figure 14 illustrates the relative error $(H^{SON}_{\sigma_w-100} - H_{ec})/H_{ec}$ as a function of the local mechanical production. It is clear that the accuracy is much better for small values than for large values, indicating that the assumption applied is in many cases not correct.

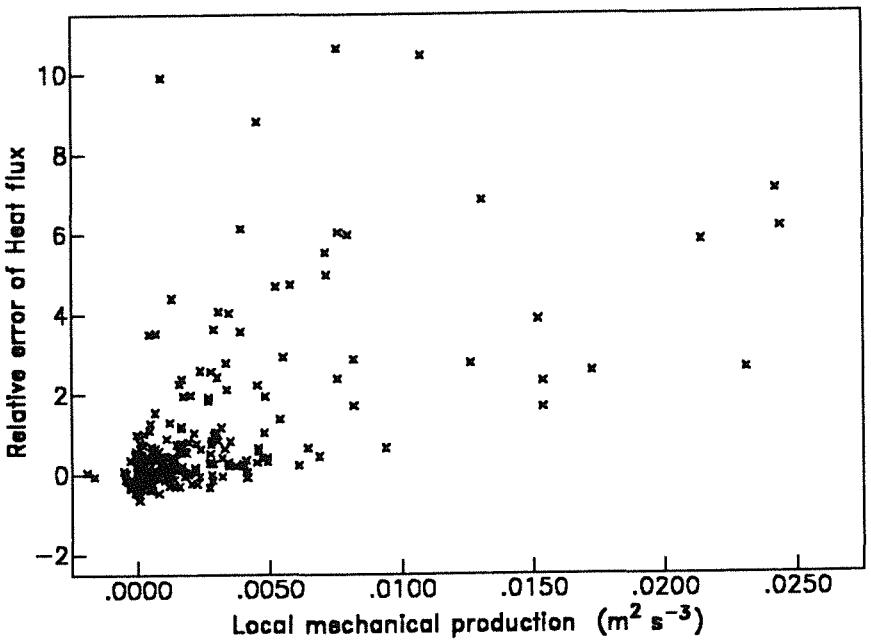

Figure 14: $(H^{SON}_{\sigma_w-100} - H_{ec})/H_{ec}$ versus local mechanical production during July 1990.

3.5.2 Tables of results

A variety of weather conditions were experienced during the two months experiment, including a bright and clear sky, partial cloud cover and overcast conditions.

The sensible heat flux estimated from each of the methods namely eddy correlation (H_{ec}), SODAR C_T^2 ($H_{C_T}^{SOD}$), and σ_w ($H_{\sigma_w-100}^{SON}$, $H_{\sigma_w-100}^{SOD}$, $H_{\sigma_w-pr}^{SOD}$) are compared in Tables 2 and 3 for the months June and July 1990. Only data corresponding to the time interval 10h00 to 19h00 CET have been used. N indicates the number of data couples, $\bar{X}$ indicates the mean value of the sensible heat flux estimate, $\bar{Y}$ and σ_Y indicate the mean value and standard deviation of the reference eddy correlation method. The basic criteria are the bias B, the root mean square error $RMSE$, the precision or standard deviation of error P, the root mean square error of calibrated data C, the slope a and Y intercept b of the regression analysis, and the correlation coefficient R. The calibrated estimated sensible heat flux (X_i') is

$$X_i' = a\,X_i + b \tag{23}$$

with a and b parameters of the regression line calculated with June 1990 data. The results give us the opportunity to check if the parameters a and b are constant and can therfore be used for a calibration of the estimates. The conclusions may be summarized as follow:

- H estimated by the C_T^2 method has the best correlation and the best overall precision.
- There is little variation between the two months in the estimation of a and b for all methods. The correlation and RMSE are also nearly the same. The parameters a and b can be used as calibration coefficients.
- The poor results of $H_{\sigma_w-100}^{SOD}$, are due to the errors when measuring σ_w by means of a SODAR. A simple linear fit of the SODAR σ_w does not seem to be sufficient. The characteristic quantities of both the PBL and the SODAR would be necessary for a better calibration of SODAR σ_w.
- All methods have their own limitations, which arise from the fact that the similarity law is not true under all atmospheric situations. In the following section, we will present a more detailed study of these limitations.

Table 2: Comparison of Heat flux estimated by the two indirect methods and the eddy correlation method during June 1990.

	$H_{C_T}^{SOD}$	$H_{\sigma_w-100}^{SON}$	$H_{\sigma_w-100}^{SOD}$	$H_{\sigma_w-pr}^{SOD}$
N	194	255	255	101
$\bar{X}(Wm^{-2})$	55	141	127	222
$\bar{Y}(Wm^{-2})$	97	100	100	88
$\sigma_Y(Wm^{-2})$	80	86	86	77
$B(Wm^{-2})$	42	-42	-27	-134
$RMSE(Wm^{-2})$	72	86	100	189
$P(Wm^{-2})$	58	76	96	132
$C(Wm^{-2})$	50	64	79	61
a	1.94	0.59	0.38	0.29
$b(Wm^{-2})$	-10	17	52	23
R	0.78	0.66	0.39	0.62

Table 3: Comparison of Heat flux estimated by the two indirect methods and the eddy correlation method during July 1990.

	$H_{C_T}^{SOD}$	$H_{\sigma_w-100}^{SON}$	$H_{\sigma_w-100}^{SOD}$	$H_{\sigma_w-pr}^{SOD}$
N	131	201	201	69
$\bar{X}(Wm^{-2})$	64	168	137	286
$\bar{Y}(Wm^{-2})$	131	121	121	123
$\sigma_Y(Wm^{-2})$	95	93	93	90
$B(Wm^{-2})$	67	-48	-16	-163
$RMSE(Wm^{-2})$	98	94	90	209
$P(Wm^{-2})$	71	80	89	132
$C(Wm^{-2})$	60	72	76	70
a	2.13	0.61	0.57	0.34
$b(Wm^{-2})$	-6	17	46	27
R	0.78	0.63	0.54	0.63

3.5.3 Time series

In this section time series of the heat flux $H_{\sigma_w-100}^{SON}$ (calculated using the sonic standard deviation of vertical wind speed), and $H_{\sigma_w-pr}^{SOD}$ and $H_{C_T}^{SOD}$ (calculated using the SODAR data), are presented in comparison with H_{ec}. Time series have been concatenated and have been corrected using the calibration parameters a and b given in Table 2. Each Figure depicts the time series of sensible heat flux in comparison to the reference value H_{ec} during one month. All the methods show that the diurnal variations are generally well followed.

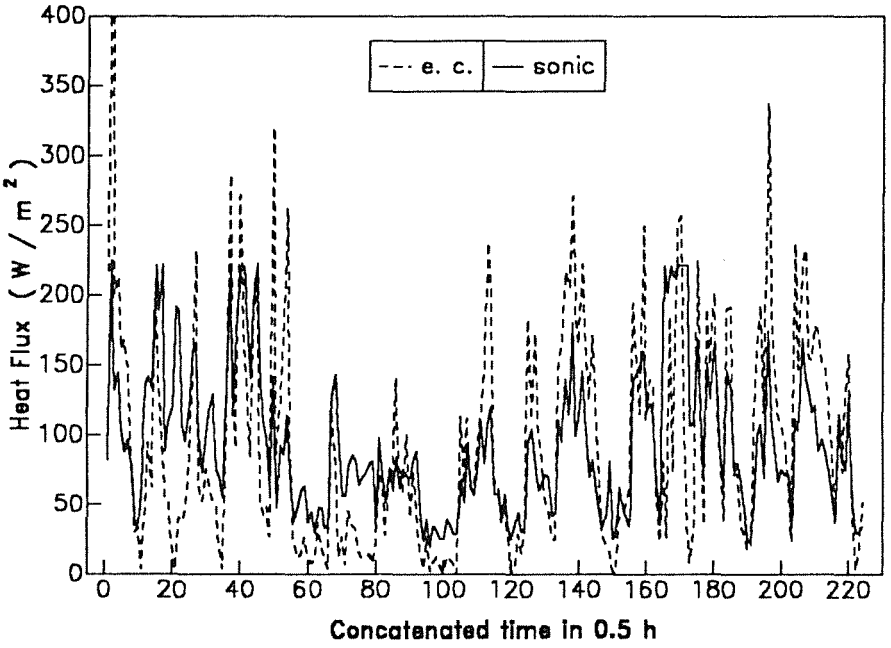

Figure 15: Time series of $H^{SON}_{\sigma_w-100}$ and reference H_{ec} during June 1990.

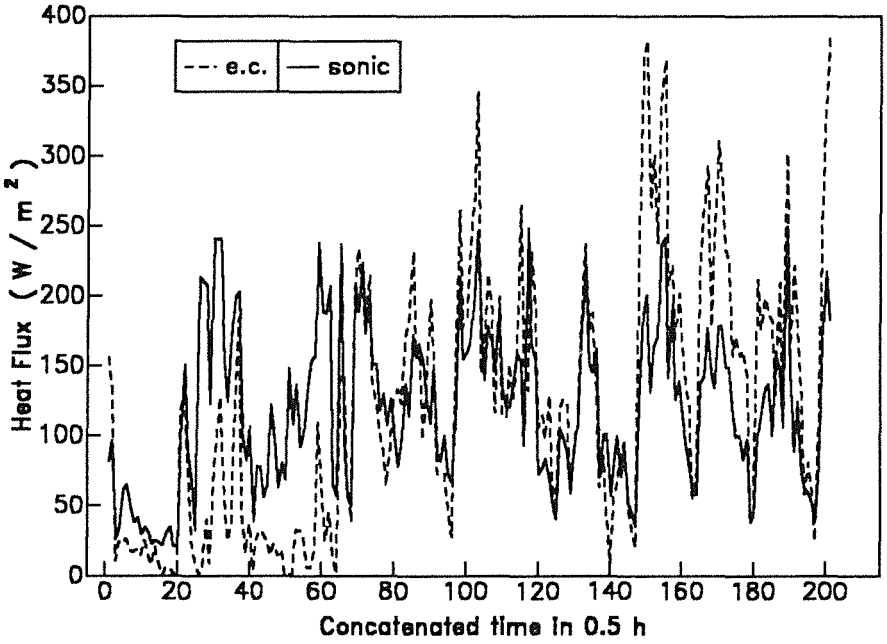

Figure 16: Time series of $H^{SON}_{\sigma_w-100}$ and reference H_{ec} during July 1990.

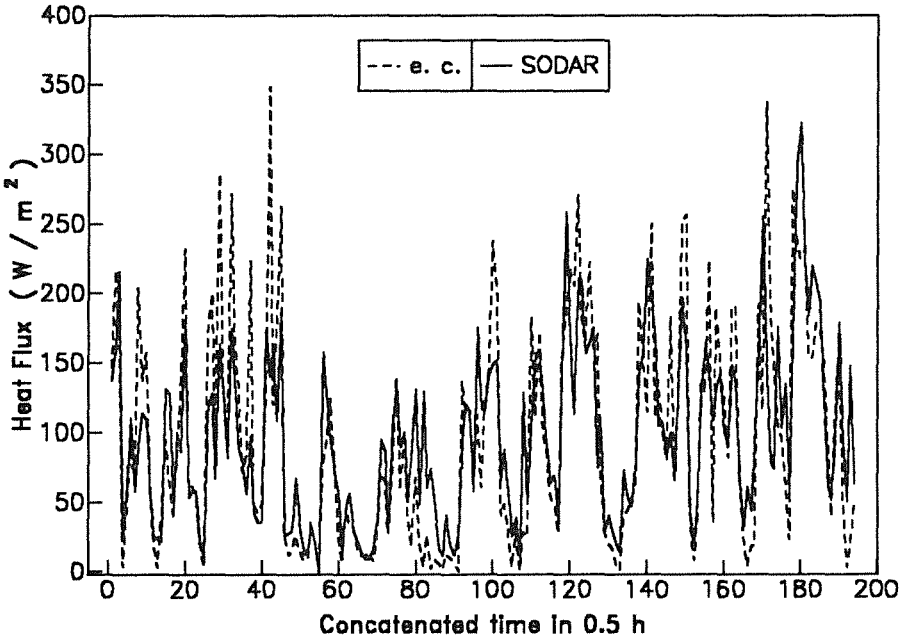

Figure 17: Time series of $H_{C_T}^{SOD}$ and reference H_{ec} during June 1990.

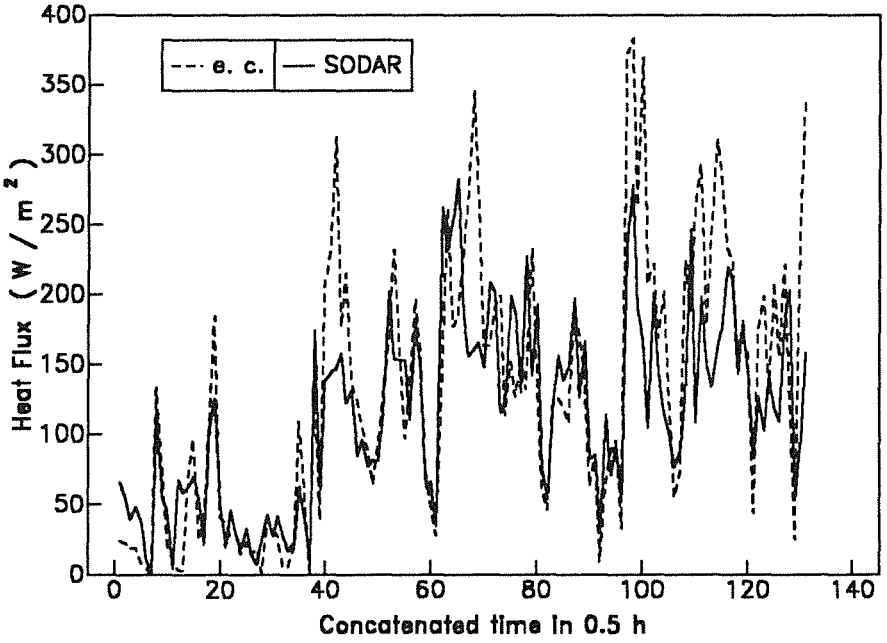

Figure 18: Time series of $H_{C_T}^{SOD}$ and reference H_{ec} during July 1990.

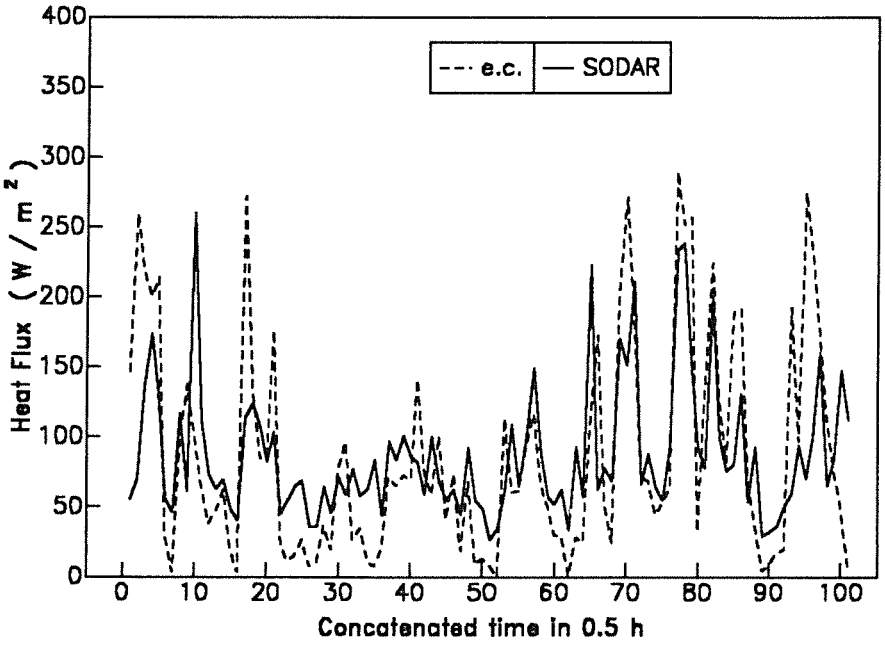

Figure 19: Time series of $H^{SOD}_{\sigma_w - pr}$ and reference H_{ec} during June 1990.

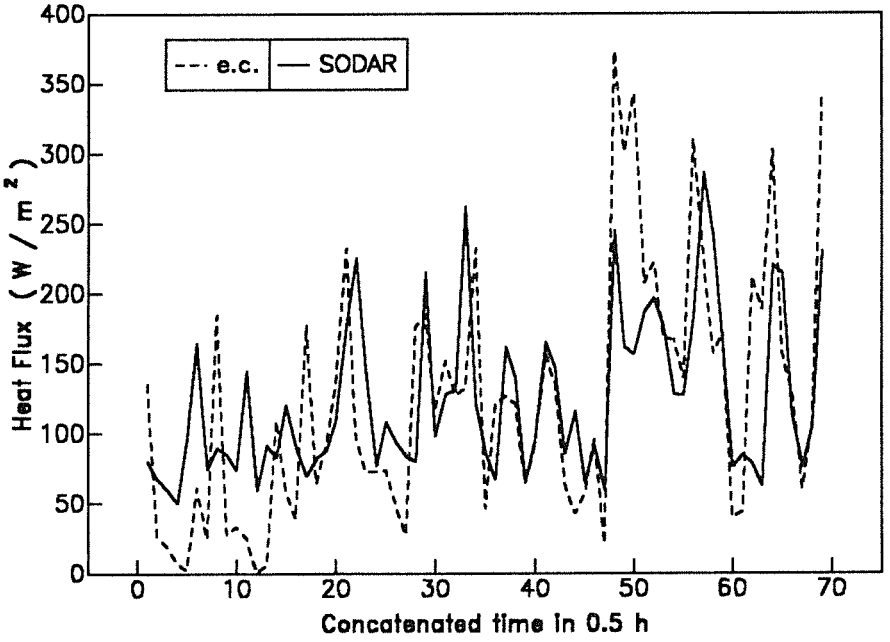

Figure 20: Time series of $H^{SOD}_{\sigma_w - pr}$ and reference H_{ec} during July 1990.

The observation of Figures 15 to 20 can be summarized as follows:

- The calculation of H using C_T^2 (Figures 17 and 18) seems to be in good agreement with the reference sensible heat flux over the course of the two months. The method using C_T^2 overestimates small values of H and underestimates large values of H. This is due to the same trend of C_T^2 as already stated in Section 2.4.3.

- Calculation of H using sonic σ_w (Figures 15 and 16) is in fair agreement with H_{ec}. But, from time to time the computation by means of σ_w overestimates greatly the reference measurement: this is due to the fact that the assumption of a negligible local mechanical production is, in such cases, not correct.

- Estimating H with SODAR σ_w profile (Figures 19 and 20) reduces the error as compared to the method of using σ_w measured at 100 m AGL only. However, in many cases, no sensible heat flux can be computed because the σ_w^3/z profile does not permit to compute the sensible heat flux with a good confidence, as indicated by the small number N in Tables 2 and 3.

3.6 Concluding remarks

The purpose of this Section was to compare two different methods for the calculation of the sensible heat flux with SODAR data. The method proposed by Coulter and Wesely (1980) using C_T^2 gives good results for convective mixed layer conditions typical of summer. The second method presented by Weil *et al.* (1980) using σ_w is also interesting because it gives estimates of the profile of the sensible heat flux within the Planetary Boundary Layer but its range of applicationis narrower than the first method.

4 Conclusion

The comparison of C_T^2 derived from SODAR and sonic anemometer-thermometer data gives similar results in convective situations. Because this parameter varies within two or more orders of magnitude in time, detected differences of a factor of 2 may not be as serious as might first appear. A test with instantaneous measurements of SODAR echo and tethered ballons instrumented with high response C_T^2 sensors would be necessary to further investigate the errors of measurement of the SODAR, and in order to precisely calibrate the SODAR in the range 200 m to 1 km AGL.

Calculation of the sensible heat flux by means of SODAR is possible with the help of the mixed layer similarity theory. Among several possible methods, we present two using respectively properties of the C_T^2 profiles and σ_w profiles of the convective PBL, and providing estimates of the sensible heat flux. Comparison of both methods with the eddy correlation method shows good agreement in most cases. Two significant advantages of the first method are: (i) It yields an estimation of the sensible heat flux and also rejects cases when the underlying assumptions are not valid. The second method does not permit to check if its underlying assumptions are valid. (ii) It can be used more often than the second method. This is because a great percentage of σ_w^3/z profiles to be used in the second method must be rejected, due to uncertainties in the SODAR measurement.

Acknowledgments

The authors thank Mr. P. Burger for his helpful comments and his assistance when using the sonic anemometer and the SODAR. Mr. K.H. Pfeffer and Ms. S. Honcu helped in the data transfer and the data processing.

We are also grateful to Dr. G. Quinn and Dr. M.Tercel from KfK-IGT who helped in the redaction of the paper and the correction of the manuscript.

References

Asimakopoulos D.N., Cole R.S., Caughey S.J. and Crease B.A., 1976: *A quantitative comparison between acoustic sounder returns and the direct measurement of atmospheric temperature fluctuations.* Bound.-Layer Meteorol., Vol. 10, 137-147.

Asimakopoulos D.N., Moulsley T.J., Helmis C.G. Lalas D.P. and Gaynor J., 1983: *Quantitative low level acoustic sounding and comparison with direct measurement.* Bound.-Layer Meteorol., Vol. 27, 1-26.

Caughey S.J., Crease B.A., Asimakopoulos D.N., and Cole R.S., 1978: *Quantitative bistatic acoustic sounding of the atmospheric boundary layer.* Quat. J. Roy. Met. Soc., Vol. 104, 147-161.

Chintawongvanich P., Olsen R. and Biltoft C.A., 1989: *Intercomparison of Wind Measurements from Two Acoustic Doppler Sodars, a Laser Doppler Lidar, and In Situ Sensors.*J Atmos. Oceanic Technol., Vol. 6, 785-797.

Clifford S.F. and Brown E.H., 1980: *Excess attenuation in echosonde signal.* J. Acous. Soc. Am., Vol 67, 6, 1967-1973.

Gentou H., Thomas P., and Vogt S., 1991: *Comparison of Turbulence Parameters Measured by SODAR and Sonic Anemometer.* KfK Report 4890, Nuclear Research Center Karlsruhe, Karlsruhe, F.R.G.

Harris C.M., 1966: *Absorption of Sound in Air Versus Humidity and Temperature.* J. Acoust. Soc. Am., Vol. 40, No. 1, 148-159.

Haugen D.A. and Kaimal J.C., 1978: *Measuring Temperature Structure Parameter Profiles with an Acoustic Sounder.* J. Appl. Meteor., Vol. 17, 895-899.

Helmis C.G., Asimakopoulos D.N., Lalas D.P. and Moulsley T.J., 1983: *On the local isotropy of the temperature field in an urban area.* J. Appl. Meteor., Vol. 22, 1594-1601.

Helmis C.G., Asimakopoulos D.N. and Cole R.S. , 1985 : *A low level atmospheric vertical velocity comparison between a high-resolution acoustic sounder and a turbulence probe.*IEEE Trans. Geosc. and rem. sensing, Vol. GE-23, No. 2, 164-170.

von Holleuffer-Kypke R., Hübschmann W.G., Süß F ., Thomas P. (1984): *Meteorologisches Informationssystem des Kernforschungszentrums Karlsruhe.*Atomkernenergie, Kerntechnik Vol 44, No.4, 300-304.

Kaimal J.C., 1972: *Turbulence spectra, length scales and structure parameters in the stable surface layer.* Bound.-Layer Meteorol., Vol. 4, 289-309.

Kaimal J.C., Wyngaard J.C., Haugen D.A., Coté O.R. and Izumi Y., Caughey S.J. and Readings C.J. , 1976 : *Turbulence Structure in the Convective Boundary Layer* . J. Atmos. Sci., Vol. 33, 2152-2169.

Kaimal J.C., Abshire N.L., Chdadwick R.B., Decker M.T., Hooke W.H., Kropfli R.A., Neff W.D. and Pasqualucci F, 1982 : *Estimating the Depth of the Daytime Convective Boundary Layer* J. Appl. Meteor., Vol. 21, 1123-1129.

Keder J., Foken Th, Gertman W. and Schinkler V., 1989: *Measurement of wind parameters and heat flux with the Sensitron Doppler sodar.* Bound.-Layer Meteorol., Vol. 46, 195-204.

Melas D, 1990: *Sodar estimates of surface heat flux and mixed layer depth compared with direct measurements.* Atmospheric Environment, Vol. 24 A, No. 11, 2847-2853.

Moulsley T.J., Asimakopoulos D.N., Cole R.S., Caughey S.J., Crease B.A., 1982: *Temperature structure parameter measurement using differential temperature sensors.* Bound.-Layer Meteorol., Vol. 23, 307-315.

Neff W.D., 1978: *Beamwidth Effects on Acoustic Backscatter in the Planetary Boundary Layer.* J. Appl. Meteor., Vol. 17, 1514-1520.

Neff W.D. and Coulter R.L., 1986: *Acoustic remote sensing.*Probing the Atmospheric Boundary Layer, edited by Lenschow D.H., AMS, Boston, Massachusetts, USA.

Schotanus P., Niewstadt F.T.M., De Bruin H.A.R., 1983: *Temperature measurement with sonic anemometer and its application to heat and moisture fluxes.* Bound.-Layer Meteorol., Vol. 26, 81-93.

Thomas P. and Vogt S., 1990: *Measurement of wind data by Doppler-SODAR and tower instruments: An intercomparison.* Meteorol. Rdsch., Vol. 42, 161-165.

Weil A., Klopsisz C., Strauss B., Baudin F., Jaupart C. , von Grunderbeeck P., Goutorbe J.P., 1980: *Measuring Heat Flux and Structure Functions of Temperature Fluctuations with an Acoustic Doppler SODAR.* J. Appl. Met., Vol. 19, 199-205.

Wyngaard J.C., Izumi J. and Collin Jr., Stuart A., 1971: *Behavior of the refractive index structure parameter near the ground* J. Opt. Soc. Am., Vol. 61, 1646-1650.